25. Transient absorption measurements on the microsecond time scale suggest that Rh(II), formed in the initial ET reaction, does not contribute significantly to the size of the transient absorption signal for the ground-state recovery of M(II) (M = Ru, Os). The amplitude of fast recovery of ground-state absorption is therefore related to the fraction of M(III) reacting to regenerate M(II).
26. R. A. Marcus and N. Sutin, *Biochim. Biophys. Acta* **811**, 265 (1985).
27. Supplementary information available (*28*). Provided are a description of the laser apparatus used for ultrafast measurements and time-resolved transient absorption data monitoring the recovery of ground-state absorption of Δ-Os(phen)$_2$dppz^{2+} in the presence of DNA and Δ-Rh(phi)$_2$bpy^{3+}.
28. The material can be accessed on the World Wide Web at http://www.science-mag.org/science/feature/beyond/#arkin and can be ordered from AAAS (see any current masthead page for ordering information).
29. Data is also available as a figure on the Web (*28*).
30. The greater accessibility of water to the DNA-bound Λ enantiomer, as suggested by its shorter excited-state lifetimes, will have some effect on the reorganization energy.
31. J. K. Barton, *Science* **233**, 727 (1986).
32. M. R. Arkin, E. D. A. Stemp, C. Turro, N. J. Turro, J. K. Barton, *J. Am. Chem. Soc.* **118**, 2267 (1996).
33. C. S. Chow and J. K. Barton, *Methods Enzymol.* **212**, 219 (1992).
34. A. Sitlani and J. K. Barton, *Biochemistry* **33**, 12100 (1994).
35. The pattern of photocleavage changes somewhat upon the addition of salt, indicating that this assay is highly sensitive to small changes in DNA structure.
36. Guanine has the lowest oxidation potential of all the bases. Therefore, if the single rate reflected oxidation of a proximal base by the oxidized donor, one would expect that the rate would be faster in poly[d(GC)], but we observe the opposite trend. Moreover, the loading-independent rate of $k_{rec} = 1 \times 10^{10}$ s^{-1} is observed for Os(phen)$_2$dppz^{3+}, for which oxidation of guanine is precluded on thermodynamic grounds [T. W. Welch, A. H. Corbett, H. H. Thorp, *J. Phys. Chem.* **99**, 11757 (1995)].
37. D. M. Crothers, *Biopolymers* **6**, 575 (1968); D. E. V. Schmechel and D. M. Crothers, *ibid.* **10**, 465 (1971).
38. M. Vorlickova and J. Kypr, *J. Biomol. Struct. Dyn.* **3**, 67 (1985); C. A. Hunter, *J. Mol. Biol.* **230**, 1025 (1993); K. Yanagi, G. G. Privé, R. E. Dickerson, *ibid.* **217**, 201 (1991).
39. We modeled the intercalation of metal complexes by loading a one-dimensional lattice with two different intercalators to simulate the distribution of separations between donors and acceptors on the DNA. For the Δ-Ru(phen)$_2$dppz^{2+}–Δ-Rh(phi)$_2$bpy^{3+} pair of reactants, experimental data on all time scales are reasonably well described by $\beta \sim 1.5$ Å^{-1} (*26*) and a preference ratio of 13 favoring nearest-neighbor cooperative binding of donor and acceptor (A. Hörmann, E. J. C. Olson, P. F. Barbara, unpublished results).
40 A. Sitlani, C. M. Dupureur, J. K. Barton, *J. Am. Chem. Soc.* **115**, 12589 (1993).
41. S. J. Atherton *et al.*, *J. Phys. Chem.* **91**, 3137 (1987).
42. D. B. Hall, R. E. Holmlin, J. K. Barton, unpublished results.
43. The subpopulation of more slowly reacting donors could be decoupled from acceptors by defects in base stacking. The finite probability of encountering such a defect, arising from DNA structural polymorphism, should increase with increasing donor-acceptor separationseparation.
44. S. Kartha, R. Das, J. R. Norris, *Met. Ions Biol. Syst.* **27**, 323 (1991); S. G. Boxer, *Annu. Rev. Biophys. Biophys. Chem.* **19**, 267 (1990).
45. H. M. McConnell, *J. Chem. Phys.* **35**, 508 (1961); C. A. Naleway, L. A. Curtiss, J. R. Miller, *J. Phys. Chem.* **95**, 8434 (1991).
46. G. L. Closs and J. R. Miller, *Science* **240**, 440 (1988); D. S. Wuttke, M. J. Bjerrum, J. R. Winkler, H. B. Gray, *ibid.* **256**, 1007 (1992); C. C. Moser, J. M. Keske, K. Warncke, R. S. Farid, P. L. Dutton, *Nature* **355**, 796 (1992); R. Langen *et al.*, *Science* **268**, 1733 (1995); G. M. Ullmann and N. M. Kostic, *J. Am. Chem. Soc.* **117**, 4766 (1995).
47. D. Dee and M. E. Baur, *J. Chem. Phys.* **60**, 541 (1974).
48. A. K. Felts, W. T. Pollard, R. A. Friesner, *J. Phys. Chem.* **99**, 2929 (1995); V. Mujica, M. Kemp, M. A. Ratner, *J. Chem. Phys.* **101**, 6856 (1994); *ibid.*, p. 6849; M. Kemp, V. Mujica, M. A. Ratner, *ibid.*, p. 5172.
49. Several authors have determined thermodynamic parameters for the DNA bases, but no consensus has yet emerged. See S. Steenken, J. P. Telo, H. M. Novais, L. P. Candeias, *J. Am. Chem. Soc.* **114**, 4701 (1992); N. S. Hush and A. S. Cheung, *Chem. Phys. Lett.* **34**, 11 (1975); M. Faraggi and M. H. Klapper, *J. Chim. Phys.* **91**, 1054 (1994); S. V. Jovanovic and M. G. Simic, *J. Phys. Chem.* **90**, 974 (1986); L. Kittler, G. Löber, F. A. Gollnick, H. Berg, *J. Electroanal. Chem.* **116** , 503 (1980).
50. L. A. Lipscomb *et al.*, *Biochemistry* **35**, 2818 (1996).
51. Transient absorption data on the nanosecond time scale were obtained with instrumentation described by M. Bacharach [thesis, California Institute of Technology (1995)] at concentrations of 67 μmM Ru and 3.4 mM DNA bp.

52. We are grateful to NIH (GM49216 to J.K.B.) and NSF (CHE-9304373 to P.F.B.) for financial support. We also thank NSF for predoctoral support of M.R.A. and R.E.H., and the American Cancer Society for postdoctoral support of E.D.A.S. We are also grateful to N. J. Turro for helpful discussions and to the reviewers for thoughtful comments.

22 November 1995; accepted 6 May 1996

Low-Frequency Raman Scattering and the Fast Relaxation Process in Glycerol

Takashi Uchino* and Toshinobu Yoko

Ab initio molecular orbital calculations were used to determine the structure and vibrational frequencies of the cyclic glycerol trimer, which represents the region of medium-range ordering in liquid and supercooled glycerol. The calculations reproduced the experimentally observed low-frequency Raman scattering peak (or the "boson peak") at ~50 per centimeter, which suggests that the peak results from the localized collective motions of the cooperatively hydrogen-bonded hydroxyl groups. The calculations also suggest that the fast relaxation process may result from the translational motion of each glycerol molecule in the cyclic structure. On the basis of these results, a model of the glass transition was developed.

The low-frequency (<~100 cm^{-1}) relaxations and vibrations in amorphous systems have been the focus of numerous studies aimed at understanding the anomalous low-temperature properties and glass transition phenomena observed in such systems (*1*). Although the relaxational part of the dynamics in supercooled liquids is well described by the mode coupling theory (MCT) (*2*), the vibrational excitations, generally called the "boson peak," cannot be explained in terms of MCT, and the origin of the boson peak is still unsettled. Thus, understanding the boson peak and the fast relaxation process near the glass transition temperature T_g remains an important goal in solid-state physics. It has recently been suggested that the atomic motions in a medium-range scale on the order of ~10 Å in amorphous solids are closely related to the boson peak (*3*). This hypothesis strongly suggests that the normal-mode analysis of molecules modeling a medium-range order (MRO) in a particular glass will shed light on the physical origin of the boson peak.

Glycerol has been widely used to investigate the low-frequency vibrational properties of liquids and supercooled liquids, because liquid glycerol is one of few systems that remain in the metastable supercooled state long enough to permit Raman scattering (*4–8*) and neutron scattering (*7*, *9*) measurements. The low-frequency Raman scattering spectra of glycerol below T_g (186 K) are characterized by a nonsymmetric boson peak with a broad maximum around 50 cm^{-1}; the peak shifts slightly to higher frequencies with decreasing temperature. Raman scattering measurements in the O–H stretching region have demonstrated that liquid and supercooled glycerol are self-associated through intermolecular hydrogen bonds to form dimer, trimer, and oligomer structures (*8*). Neutron diffraction measurements (*9*) have demonstrated that liquid glycerol not only has intramolecular correlations but also exhibits some residual structure in the intermediate range (2 to 6 Å). These findings indicate that, despite the flexibility of each molecular unit, the intermolecular distribution function exhibits significant structural ordering as a result of intermolecular hydrogen bonding.

Although the exact intermolecular conformation of the MRO in glycerol has not been determined, it has been demonstrated that small water (*10*) and methanol (*11*, *12*) clusters tend to form cyclic hydrogen-bonded trimers. The intermolecular hydrogen bonds in such trimers are considered to be enhanced by cooperative

---

Institute for Chemical Research, Kyoto University, Uji, Kyoto 611, Japan.

*To whom correspondence should be addressed.

effects; that is, each molecule of the complex acts not only as a donor but also as an acceptor of hydrogen bonds. Thus, it is reasonable to assume that in liquid and supercooled glycerol a cyclic trimer structure also exists, yielding a well-defined MRO. We do not mean to imply that chainlike forms of the glycerol dimer, trimer, and oligomers do not exist in real liquids; rather, we assume that the cyclic trimer is the most likely structure underlying the MRO in liquid and supercooled liquid glycerol (*13*). Therefore, we have calculated harmonic vibrational frequencies of some cyclic glycerol trimers to test the hypothesis that, if the boson peak results primarily from the vibrational excitation of MRO in a supercooled liquid, then an isolated cluster modeling the MRO should have normal modes with frequencies that match those of the observed boson peak.

We performed a full-geometry optimization in the $3N - 6$ (N = number of atoms) internal coordinates space for the cyclic glycerol trimer. Because of the size of the system, we performed the calculations only at the Hartree-Fock (HF)/6-31G level (*14*) using the Gaussian 94 computer program (*15*). In the optimized geometry of the glycerol trimer (model I) (Fig. 1), the three glycerol molecules are almost equivalent to each other, resulting in a C_3-like structure (*16*). All OH groups participate in cooperative hydrogen bonds to form two rings: the inner 6-membered ring, consisting of three intermolecular hydrogen bonds, and the outer 12-membered ring, consisting of three intramolecular and three intermolecular hydrogen bonds. The intermolecular O···H bond distance in the outer ring (~1.77 Å) is shorter than that in the inner ring (~1.87 Å), which indicates that the outer hydrogen bonds are stronger than the inner ones. The association energy obtained by the simple difference between the total energies of the trimer and its constituent molecules was calculated to be −172.48 kJ mol^{-1} (*17*). Thus, model I can be regarded as a highly stable conformation, representing one of the possible forms of the glycerol trimer.

Using this optimized geometry, we calculated the harmonic vibrational frequencies at the HF/6-31G level (Table 1). Force constants were obtained by the gradient method (*18*), and Raman scattering intensities were calculated according to the procedure of Frisch *et al.* (*19*). No imaginary frequency was obtained for model I, which demonstrated that model I is a stationary point such that the forces on the system are essentially zero. It is generally accepted that single-determinant wave functions yield too steep a potential in the vicinity of the equilibrium structure and that the theoretical frequencies at the HF level are consistently larger than the experimental harmonic val-

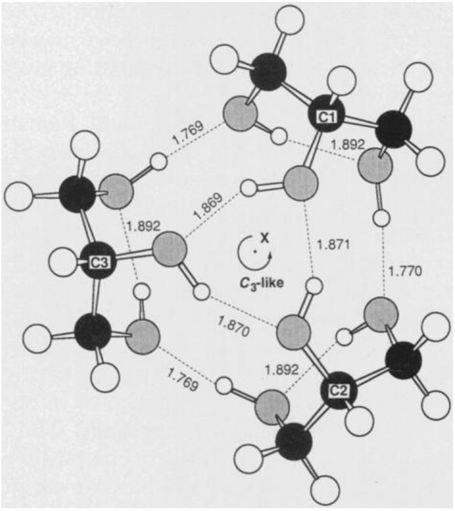

Fig. 1. Hartree-Fock 6-31G optimized structure for the glycerol trimer (model I). In this and subsequent figures, solid, shaded, and white spheres represent carbon, oxygen, and hydrogen atoms, respectively. Hydrogen bonds are indicated by broken lines, and their distances are shown in angstroms. X–C1 = X–C2 = X–C3 = 3.124 Å.

Table 1. Vibrational frequencies ν, reduced masses m, force constants k, and Raman scattering intensities I of the modes less than 100 cm^{-1} calculated for model I at the HF/6-31G level.

ν (cm^{-1})	m (amu)	k (mdyne Å^{-1})	I (Å^4 amu^{-1})
51.06	5.2775	0.0081	0.0458
51.13	5.2791	0.0081	0.0457
77.09	6.3255	0.0221	0.0841
77.13	6.3204	0.0222	0.0842
93.09	5.6635	0.0289	0.0039
94.96	4.0484	0.0215	0.1606
95.06	4.0429	0.0215	0.1602

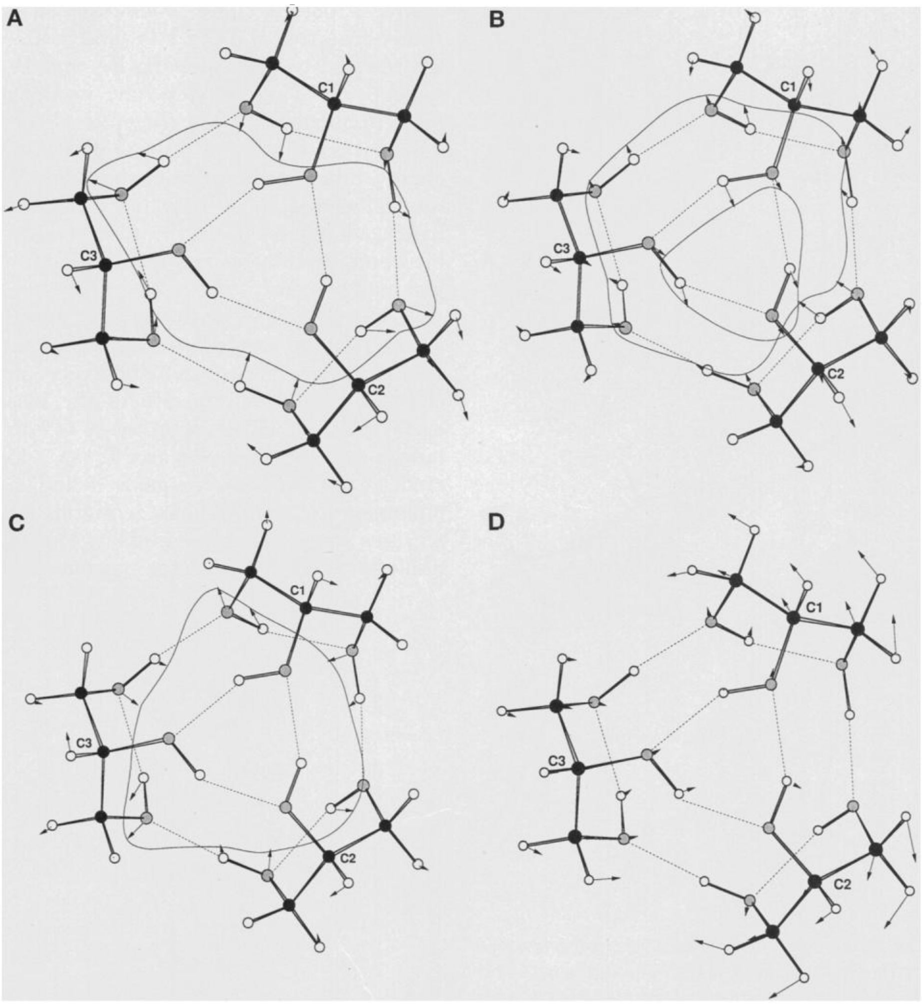

Fig. 2. The vector displacements of the low-frequency vibrational modes at (**A**) 51.06 cm^{-1}, (**B**) 77.09 cm^{-1}, (**C**) 93.09 cm^{-1}, and (**D**) 94.96 cm^{-1} calculated for model I. Hydrogen bonds are indicated by broken lines. The solid lines in (A), (B), and (C) link the ends of the vectors, showing the localized collective motions of the cooperatively hydrogen-bonded OH groups to form a sort of "standing wave."

ues by ~10% (*20*). However, we did not scale the calculated frequencies using the empirical factor because the absolute deviations are expected to be small (at most ~10 cm^{-1}) for these low-frequency vibrational modes.

There are two kinds of vibrational modes for model I (Fig. 2). The modes at ~51, ~77, and ~93 cm^{-1} (Fig. 2, A to C) are mainly attributable to the motions of the OH groups, whereas the modes at ~95 cm^{-1} (Fig. 2D) result from the translational motions (especially those of the CH_2 and CH groups) in each glycerol molecule. The former vibrational modes can be described as "standing waves" of the inner 6-membered or the outer 12-membered rings; the OH groups in these rings thus can oscillate according to specific periodic boundary conditions as if they were connected by elastic springs or by hydrogen bonds. On the other hand, the vibrations at ~95 cm^{-1} involve large displacements of outer atoms and should therefore depend strongly on the trimer surroundings. These results strongly indicate that the cyclic glycerol trimer yields the collective localized vibrations in the low-frequency (<100 cm^{-1}) region.

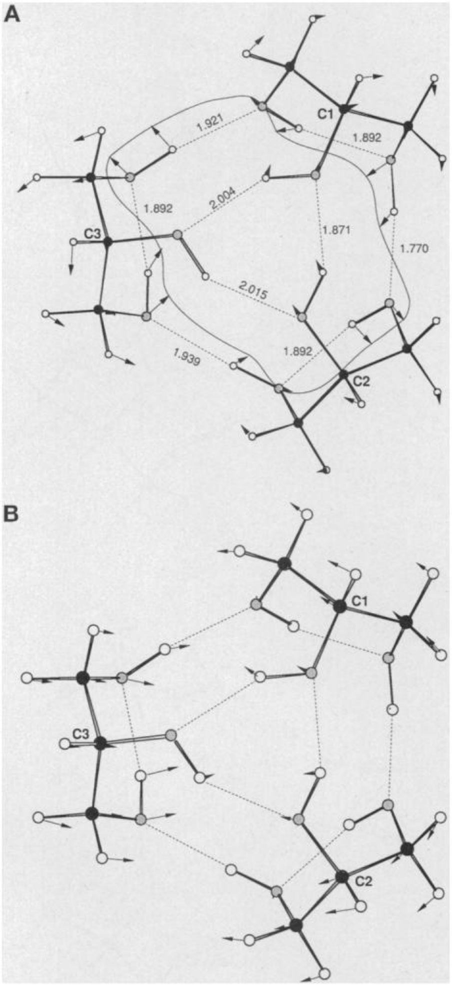

Fig. 3. The vector displacements of the low-frequency vibrational modes at (**A**) 49.07 cm^{-1} and (**B**) 84.75 cm^{-1} calculated for model IV, which can be compared with Fig. 2, A and D, respectively. Hydrogen bonds are indicated by broken lines, and their distances are shown in angstroms. The solid lines represent the "standing waves."

Although model I is likely to capture some fundamental features of the MRO in liquid and supercooled liquid glycerol, the glycerol trimer will not always have such an ideal cyclic conformation in real liquids. We therefore investigated the effect of deformation of the ideal cyclic structure on the vibrational frequencies. We calculated energy variations of model I as a function of the X–C3 distance in Fig. 1, where X is the isodistant point from the C1, C2, and C3 atoms, while fixing the X–C1 and X–C2 distances, the C1–X–C2, C2–X–C3, and C3–X–C1 angles, and the other intramolecular parameters at their optimized values. We then carried out the frequency calculations for each deformed cyclic structure. The complexes with X–C3 distances of 3.20, 3.25, and 3.30 Å are referred to as models II, III, and IV, respectively. These models have no imaginary frequency and can therefore also be regarded as stationary points. The total energy difference between models I and IV was calculated to be only 6.5 kJ mol^{-1}; hence, all these clusters represent probable conformations as the trimer structure in liquid glycerol.

Comparing Fig. 2 with Fig. 3, A and B, we see that the vector displacements of the low-frequency modes are effectively unchanged by the deformation of the ideal cyclic structure. However, as the X–C3 distance increases, the modes at ~95 cm^{-1} for model I shift to lower frequencies and, simultaneously, their Raman scattering intensities abruptly decrease (see Fig. 4). This result indicates that the force constants and the first derivatives of the polarizability with respect to nuclear coordinates—which affect vibrational frequencies and Raman intensities, respectively, for these translational motions (see Figs. 2D and 3B)—are strongly dependent on the intermolecular conformation, and that the vibrational softening mentioned above occurs as the structure of the glycerol trimer deviates from the ideal cyclic conformation. Because the detailed atomic conformations vary rapidly with time in real liquids, the lifetime of these intermolecular motions is expected to be very short. As a result, these translational motions can be overdamped and can be observed on the time scale of Raman scattering measurements (<~10^{-12} s or frequency >~5 cm^{-1}) as the fast relaxation. Such a fast relaxation of the intermolecular motion can be associated with the so-called "β-relaxation" process of MCT (*1*, *2*) and is also expected to occur outside the cyclic trimer, namely, in the disordered region. However, because the vibration at ~95 cm^{-1} may depend strongly on the trimer surroundings, the suggested microscopic picture of the fast relaxation process may be significantly modified by neighboring glycerol molecules.

In contrast, the positions and Raman scattering intensities of the modes at ~51, ~77, and ~93 cm^{-1} calculated for model I are only weakly affected by the change in the intermolecular conformation. It is thus probable that these modes, all of which represent the collective motions of the hydrogen-bonded rings (see Figs. 2, A to C, and 3B), can survive without damping within a time scale of the Raman scattering measurements, yielding a broad peak as observed by the Raman spectroscopy. Thus, our results allow us to suggest one possible microscopic picture for the boson peak in glycerol, namely that it originates from the collective wavelike motions of atoms localized in the extent of its trimer structure.

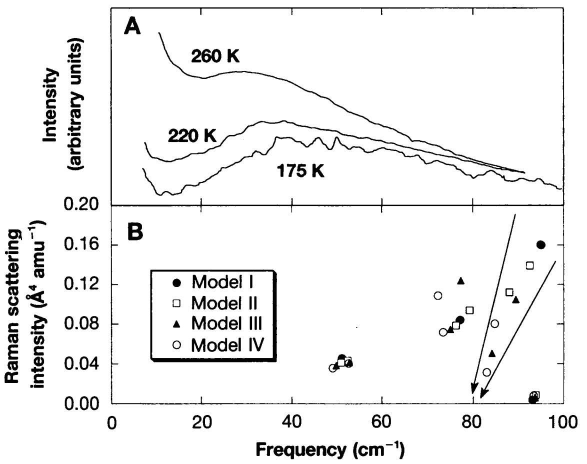

Fig. 4. (**A**) Experimental Raman spectra of glycerol observed at different temperatures (*5*). (**B**) Calculated low-frequency Raman spectra for models I, II, III, and IV at the HF/6-31G level. The arrows show the changes in the frequencies and Raman scattering intensities of the intermolecular translational modes.

This does not exclude the possibility that larger structural fragments (such as tetramers and pentamers) can also contribute to the low-frequency vibrational spectrum around the boson peak.

On the basis of these results, the following model of the glass transition of glycerol can be proposed. At temperatures far above T_g (186 K), the lifetime of the MRO or the cyclic glycerol trimer is expected to be too short to be underdamped on the time scale of the boson peak frequency ($\sim 10^{-12}$ s), and therefore only relaxation processes contribute to the dynamics of the system. As the system is cooled, the thermal excitation of atoms is suppressed, and, accordingly, the atoms in the MRO undergo collective motions on the time scale of low-frequency vibrations to yield a boson peak. In other words, a transition from relaxational (overdamped) to vibrational (underdamped) collective molecular motion occurs.

According to MCT, a blocking of the viscous flow at a critical temperature T_c is predicted (*2*). Such a blocking is probably caused by the formation of MRO with lifetimes that are long enough to generate vibrational motions. This interpretation is consistent with the observation that the temperature at which overdamping of the low-frequency vibrations occurs is essentially the same as the T_c predicted by the MCT (*21*). Although the boson peak tends to become dominant with decreasing temperature below T_c, the fast β-relaxation process persists. This is so because the intermolecular translational motions of each glycerol molecule can be overdamped even on a time scale of $\sim 10^{-12}$ s. If the system is rapidly quenched, the configuration of the MRO will be preserved to form a metastable glass phase, whereas if it is cooled very slowly, the locally stable MRO will be reorganized, resulting in the thermodynamic phase transition or crystallization (*22*).

The above model can be applied not only to the present molecular system but also to strong glass formers [in Angell's classification (*23*)] such as SiO_2 and B_2O_3 glasses. We recently carried out ab initio molecular orbital calculations on the clusters that model the MRO in B_2O_3 glass and have shown that these model clusters also yield localized vibrational modes in the low-frequency region, in good accord with experimental results (*24*).

REFERENCES AND NOTES

1. See, for example, C. A. Angell, *Science* **267**, 1924 (1995); F. H. Stillinger, *ibid.*, p. 1935; B. Frick and D. Richter, *ibid.*, p. 1939.
2. W. Götze, in *Liquids, Freezing, and the Glass Transition*, J. P. Hansen, D. Levesque, J. Zinn-Justin, Eds. (North-Holland, Amsterdam, 1991), p. 287.
3. M. Krüger, M. Soltwisch, I. Petscherizin, D. Quitmann, *J. Chem. Phys.* **96**, 7352 (1992); Z. Pan, D. O. Henderson, S. H. Morgan, *ibid.* **101**, 1767 (1994); V. N. Novikov, E. Duval, A. Kisliuk, A. P. Sokolov, *ibid.* **102**, 4691 (1995).
4. C. H. Wang and R. B. Wright, *ibid.* **55**, 1617 (1971).
5. V. Z. Gochiyaev, V. K. Malinovski, V. N. Novikov, A. P. Sokolov, *Philos. Mag. B* **63**, 777 (1991).
6. E. Rössler, A. P. Sokolov, A. Kisliuk, D. Quitmann, *Phys. Rev. B* **49**, 14967 (1994); S. Kojima, *ibid.* **47**, 2924 (1993).
7. J. Wuttke *et al.*, *Phys. Rev. Lett.* **72**, 3052 (1994); F. Fujara, W. Petry, R. M. Diehl, W. Schnauss, H. Sillescu, *Europhys. Lett.* **14**, 563 (1991).
8. S. Kojima, *J. Mol. Struct.* **294**, 193 (1993).
9. M. Garawi, J. C. Dore, D. C. Champeney, *Mol. Phys.* **62**, 475 (1987).
10. N. Pugliano and R. J. Saykally, *Science* **257**, 1937 (1992); M. Schütz, T. Bürgi, S. Leutwyler, H. B. Bügi, *J. Chem. Phys.* **99**, 5228 (1993); S. S. Xantheas and T. H. Dunnin Jr., *ibid.* **98**, 8037 (1993).
11. F. Huisken and M. Stemmler, *Chem. Phys. Lett.* **144**, 391 (1988); O. Mó, M. Yáñez, J. Elguero, *J. Mol. Struct. (Theochem.)* **314**, 73 (1994).
12. D. Peeters and G. Leroy, *J. Mol. Struct. (Theochem.)* **314**, 39 (1994).
13. As the MRO in glycerol, much larger structures such as the cyclic tetramer and pentamer are also probable; but in this work we concentrated on the vibrational properties of the cyclic trimer. Even if such larger structures are present in real liquids, our general observations and conclusions should remain valid.
14. W. J. Hehre, R. Ditchfield, J. A. Pople, *J. Chem. Phys.* **56**, 2257 (1972).
15. M. J. Frisch *et al.*, *Gaussian 94, Revision B 3* (Gaussian Inc., Pittsburgh, 1995).
16. In the strict sense, the trimer has a C_1 structure. We have confirmed that the total energy obtained for the present optimized cluster is lower than that calculated for the cluster assuming an ideal C_3 symmetry.
17. The energy obtained (-172.48 kJ mol^{-1}) is almost twice that calculated for the methanol trimer at the same level of theory [-92 kJ mol^{-1} (*10*)]. This is not surprising because the number of intermolecular hydrogen bonds in the glycerol trimer is six, whereas that in the methanol trimer is three.
18. P. Pulay, *Mol. Phys.* **17**, 197 (1969).
19. M. J. Frisch, Y. Yamaguchi, J. F. Gaw, H. F. Schaefer III, J. S. Binkley, *J. Chem. Phys.* **84**, 531 (1986).
20. W. J. Hehre, L. Radom, P. v. R. Schleyer, J. A. Pople, *Ab Initio Molecular Orbital Theory* (Wiley, New York, 1986), p. 233.
21. A. P. Sokolov, A. Kisliuk, D. Quitmann, A. Kudlik, E. Rössler, *J. Non-Cryst. Solids* **172–174**, 138 (1994).
22. The structures and energies of molecular oligomers abstracted from their crystal structures are, in general, not expected to be optimum for the isolated oligomers [see, for example, D. E. Williams and Y. Xiao, *Acta Crystallogr.* **A49**, 1 (1993)].
23. C. A. Angell, *J. Phys. Chem. Solids* **49**, 863 (1988).
24. T. Uchino and T. Yoko, *J. Chem. Phys.*, in press.
25. We thank the Supercomputer Laboratory, Institute for Chemical Research, Kyoto University, for providing the computer time and for permission to use the Cray Y-MP2E/264 supercomputer.

11 April 1996; accepted 31 May 1996

Crystalline Ropes of Metallic Carbon Nanotubes

Andreas Thess, Roland Lee, Pavel Nikolaev, Hongjie Dai,
Pierre Petit, Jerome Robert, Chunhui Xu, Young Hee Lee,
Seong Gon Kim, Andrew G. Rinzler, Daniel T. Colbert,
Gustavo E. Scuseria, David Tománek, John E. Fischer,
Richard E. Smalley*

Fullerene single-wall nanotubes (SWNTs) were produced in yields of more than 70 percent by condensation of a laser-vaporized carbon-nickel-cobalt mixture at 1200°C. X-ray diffraction and electron microscopy showed that these SWNTs are nearly uniform in diameter and that they self-organize into "ropes," which consist of 100 to 500 SWNTs in a two-dimensional triangular lattice with a lattice constant of 17 angstroms. The x-ray form factor is consistent with that of uniformly charged cylinders 13.8 ± 0.2 angstroms in diameter. The ropes were metallic, with a single-rope resistivity of $<10^{-4}$ ohm-centimeters at 300 kelvin. The uniformity of SWNT diameter is attributed to the efficient annealing of an initial fullerene tubelet kept open by a few metal atoms; the optimum diameter is determined by competition between the strain energy of curvature of the graphene sheet and the dangling-bond energy of the open edge, where growth occurs. These factors strongly favor the metallic (10,10) tube with C_{5v} symmetry and an open edge stabilized by triple bonds.

Carbon nanotubes, originally discovered as a by-product of fullerene research (*1*, *2*), are attracting increasing interest as constituents of novel nanoscale materials and device structures (*3*). Defect-free nanotubes—essentially, giant linear fullerenes—are expected to have remarkable mechanical properties, as well as electronic and magnetic properties that are in principle tunable by varying the diameter, number of concentric shells, and chirality of the tube (*4*). Further progress toward the use of nanotubes as practical materials will require the elimination of defects and other reaction products (such as amorphous carbon and catalyst particles), production in high yield, and synthetic control of tube diameter, length, chirality, and number of concentric shells.

SWNTs have been produced in the outflow of a carbon arc (*2*, *5*) and in much higher yield by laser vaporization of a graphite rod in an oven at 1200°C (*6*); in each case, a small amount of transition